Arabian Journal for Science and Engineering (2018) 43:6245–6259
https://doi.org/10.1007/s13369-018-3441-6

RESEARCH ARTICLE - CHEMICAL ENGINEERING

Green Synthesis of Phytogenic Magnetic Nanoparticles and Their Applications in the Adsorptive Removal of Crystal Violet from Aqueous Solution

Imran Ali[1] · Changsheng Peng[2,3] · Zahid M. Khan[4] · Muhammad Sultan[4] · Iffat Naz[5]

Received: 20 March 2018 / Accepted: 4 July 2018 / Published online: 12 July 2018

Abstract
An environment-friendly and cost-effective green recipe is employed for the production of green/phytogenic magnetic nanoparticle (PMNPs). Surfaces of PMNPs were functionalized by 3-mercaptopropionic acid (3-MPA) to investigate elimination performance of toxic dye, i.e., crystal violet (CV) from wastewater. Fabrication of functionalized PMNPs by 3-MPA (3-MPA@PMNPs) was characterized by various well-known techniques. Adsorption of CV onto 3-MPA@PMNPs has been experimentally investigated. The developed material showed high adsorptive rate (98.57% CV removal within 120 min) and adsorptive capacity (88.65 mg/g at 25 °C). Moreover, various adsorption isotherm and kinetic models were applied to explore probable removal mechanism. Langmuir isotherm model successfully represented adsorption equilibrium of CV onto 3-MPA@PMNPs. Further, the adsorption kinetic data harmonized reasonably with pseudo-second-order model which revealed that the removal was mainly corroborated by the mechanisms of ion-exchange and/or chemisorption. Values of thermodynamic parameter (ΔG^{o}) were −5123.37, −5313.46, −6216.23, −6764.21 and −8548.97 KJ/mol, respectively, in the temperature range from 298.15 to 333.15 K. While the values of ΔH^{o} and ΔS^{o} were −47.44 and −8.67 KJ/mol, respectively. These values show that sorption was favorable, spontaneous and exothermic. The high adsorptive removal persisted at wide pH range of 6.0–12.0. The material indicated high selectivity in the presence of co-existing ions (Pd^{2+} and Cd^{2+}) and offered fastest separation times from aqueous solutions due to their superparamagnetic nature. Recovered adsorbent was re-employed for > 5 times with removal efficiency of > 85%. It is concluded that 3-MPA@PMNPs can be applied as alternative sorbent for cost-effective treatment of cationic dyes from textile wastewater.

Keywords Phytogenic magnetic nanoparticles · Characterization · Adsorptive removal · Crystal violet · Aqueous solutions

1 Introduction

Management of water pollution is a hot issue of twenty-first century, especially developing and underdeveloped economies. Water contamination is growing rapidly due to the release of synthetic dyes and hazardous wastes into natu-

Electronic supplementary material The online version of this article (https://doi.org/10.1007/s13369-018-3441-6) contains supplementary material, which is available to authorized users.

✉ Changsheng Peng
pcs005@ouc.edu.cn; cspeng@ouc.edu.cn

✉ Muhammad Sultan
muhammadsultan@bzu.edu.pk

Imran Ali
aliimran@stu.ouc.edu.cn

Iffat Naz
iffatkhattak@yahoo.com

[1] College of Environmental Science and Engineering, Ocean University of China, Qingdao 266100, China

[2] The Key Lab of Marine Environmental Science and Ecology, Ministry of Education, Ocean University of China, Qingdao 266100, China

[3] School of Environmental and Chemical Engineering, Zhaoqing University, Zhaoqing 526061, China

[4] Department of Agricultural Engineering, Bahauddin Zakariya University, Bosan Road, Multan 60800, Pakistan

[5] Department of Biology, Deanship of Educational Services, Qassim University, Buraidah 51452, Kingdom of Saudi Arabia

ral water environment without proper treatment [1,2], due the rapid industrialization and urbanization [3]. Different kinds of industries, e.g., leather, cosmetic, textile, food, and pharmaceutical, are discharging untreated toxic and aromatic pollutants into water bodies. Further, the textile industry is mainly involved in the use of synthetic/toxic dyes for coloring purpose [4]. These toxic dyes are creating serious harmful effects and diseases in the vicinity and damaging aquatic life, owing to their non-biodegradable nature [5]. Hence, the treatment of these toxic dyes prior to discharge is highly desirable. However, the removal of these dyes is not so easy because of their synthetic origin and complex molecular structure. Moreover, the elimination of these recalcitrant dyes is mainly depended on its physical and chemical characteristics, in addition to the selected treatment alternatives. The effective eradication of dyes is still an open challenge for wastewater treatment experts as the most of the technologies are costly and have deleterious effects on corresponding environment [6].

From the above perspective, various physical, chemical (coagulation, flocculation, electrochemical oxidation, chemical precipitation, ion-exchange, electrodialysis) and biological (trickling filter, activated sludge system, membrane bioreactors, biosorption, photo-catalytic degradation etc.) technologies have been utilized for the elimination of toxic dyes [1,7]. However, due to high installation and operational costs, production of substantial amount of toxic biomass and low treatment performance are the main impediments to extend these technologies for low-economy countries [1]. In contrast, adsorption process is assumed relatively far better than other in term of convenient operation, cost-effectiveness, design simplicity, high performance and low energy demand [8]. In recent years, different kinds of adsorbents have been fabricated and engaged for the treatment of these toxic dyes, including banana pith, orange peel [9], rice husk [10], peanut hull [11], coir pith [12], pinewood and jute fiber [13], zeolites, ion-exchange resins, red mud, activated carbon and composite materials [1]. Nonetheless, specific attributes such as slow kinetics, low adsorptive capacity, regeneration and reusability, the involvement of high costs in the preparation and activation of adsorbents are the hurdles in the acceptance of the technology. Hence, adsorbents with high adsorptive capacity, easy to separation and regeneration, high reusability and low cost required for fabrication are still market demanded. Currently, metal oxide nanoparticles (NPs) are getting much research attention because of their easy manufacturing, greater magnetic permeability and high stability [14,15]. These have also been used to remove and degrade these dyes from wastewater owing to their sole physical, catalytic and chemical properties. Various types of manufacturing techniques, i.e., chemical co-precipitation, micro-emulsion, electrochemical and sol–gel have been well elaborative to prepare these metal oxides NPs [1]. However, these methods are facing serious challenges because of the application of high pressure and temperature, toxic and hazardous chemicals, and abrasive reaction atmosphere in the fabrication of these metal oxides NPs [1,2]. Thus, because of these drawbacks, green nanotechnology has come into play their role these days in water treatment industry. It is using non-toxic chemicals, i.e., plant bio-molecules as reducing and capping agent [16]. Green nanotechnology is an inexpensive option and requires low temperature and pressure to prepare metal oxide NPs [17]. Furthermore, steric stabilization of metal oxides NPs can be achieved against aggregation which would eventually reduce the concerns associated to the exploitation of noxious, corrosive and flammable chemical, i.e., $NaBH_4$. Presently, various kinds of plants and plant's parts have been used to prepare green magnetic NPs and their treatment performances have also been discussed in the previously by same research group [1]. Most of them have also been employed to eliminate heavy metals (i.e., Cr, Hg, Pb As, Ni and Cd) from wastewaters [18–27]. However, very limited reports are available on the adsorptive removal of toxic dyes [7,28–30], irrespective of the fact that different kinds of green magnetic NPs were prepared by various types of plant extract and utilized for the degradation of toxic dyes. Therefore, presently PMNPs were synthesized by leafs extract of *F. chinensis Roxb*, and further the surface of PMNPs was functionalized by 3-mercaptopropionic acid (3-MPA) ligand (3-MPA@PMNPs) to achieve adsorption of toxic dye, i.e., Crystal violet (CV).

2 Materials and Methods

2.1 Materials and Chemicals

Various different types of chemicals were used in the present research investigation, as details are given in supplementary information (**Text-SI**). Further, the information regarding toxic CV dye used in the adsorption experiments is enlisted in the supplementary information (Table-SI)

2.2 Preparation of 3-Marcaptopropanic Acid Functionalized Phytogenic Magnetic Nanoparticles (3-MPA@PMNPs)

Leafs extract of *'F. chinensis Roxb'* was used to prepare PMNPs, according to authors previously published report [3,31]. Briefly, 50 mL of leafs extract and 50 mL of metal salt solution was mixed together. The mixture was heated and stirred at 80 °C and 100 rpm, respectively, for 60 min, by keeping mixture pH stable at 12 until mixture color turned to black. After this, the black color grains were separated and dehydrated for 20 min at 80 °C. Thereafter, for the functionalization, an amount of 0.50 g PMNPs and 2.354 g

3-MPA was combined mutually via sonication for 12 h in 50 mL distilled water at temperature 25 °C and pH 8. After this, the functionalized particles were picked and polished twice using ethanol solution, and then oven-dried for 20 min at 80 °C. The obtained black particles 3-Marcaptopropanic acid functionalized phytogenic magnetic nanoparticles (3-MPA@PMNPs) were used further in adsorptive experiments.

2.3 Characterization of 3-Marcaptopropanic Acid Functionalized Phytogenic Magnetic Nanoparticles (3-MPA@PMNPs)

Different kinds of instrumentations were utilized to ensure smooth functionalization and characterization of 3-MPA@PMNPs, as details are given in supplementary information (Text-SII).

2.4 Adsorption and Desorption Experiments

For the evaluation of adsorptive performance, batch experiments were conducted by stirring Erlenmeyer flasks under room temperature 25 °C at constant pH 6.5 and stirred at 100 rpm. The dosages of 3-MPA@PMNPs were optimized by varying initial dosages from 0.10 to 1.50 g/L in 25 mg/L CV dye concentration (50 mL). The effect of mixture pH was investigated in batch mode at different pH (varies from 2 to 12). A fixed quantity of 0.50 g/L powdered 3-MPA@PMNPs was inserted in an Erlenmeyer flask containing 50 mL of dye solutions (25–1000 mg/L) for the estimation of sorption isotherm, kinetic and thermodynamic parameters to assess the possible removal of CV by 3-MPA@PMNPs (**Text-SIII**). The aqueous dyes concentration was determined at the end of 15, 30, 60, 120, 180, 240, 300 and 360 min. The adsorption performance was also calculated at a different temperature of 298.15, 303.15, 313, 323.15 and 333.15 K, respectively. UV–vis spectrophotometer was employed to estimate the final concentration values of CV dye and their absorbance readings were checked at $\lambda_{max} = 585$ nm. Lastly, the removal efficiency and adsorption amount was determined by Eqs. (1) and (2).

$$\text{Removal efficiency}\,(\%) = \frac{C_o - C_t}{C_o} 100 \tag{1}$$

$$\text{Adsorption amount}, q_e\,(\text{mg/g}) = \frac{(C_o - C_e)\,V}{M} \tag{2}$$

where C_o, C_t and C_e are the initial, final and equilibrium concentration (mg/L) of dye at various time interval and saturation, respectively. Further, M (g) is the weight of the sorbent and V (L) is the amount of the dye solution.

Reusability of the prepared sorbent was investigated up to ten consecutive treatment cycles to assess the potential of 3-MPA@PMNPs for long-term applications. First, a fixed quantity of 0.500 g/L of sorbent was inserted into 25 mg/L dye and subsequently, 20 mL of 0.1M EDTA regeneration solution was added for CV dye desorption. In each cycle desorbed 3-MPA@PMNPs was completely rinsed to neutrality by DI and then re-employed for adsorption of CV dye. Equation (3) was used to calculate the desorption efficiency as given by:

$$\text{Desorption efficiency}, \eta\,(\%) = \frac{M_{\text{desorbed}}}{M_{\text{sorbed}}} 100 = \frac{(C_r V_r)}{(C_o - C_e)\,V} 100 \tag{3}$$

where M_{desorbed} and M_{sorbed} are the amount of dye (mg/g) sorbed by and desorbed from sorbent, respectively. C_r (mg/L) is the concentration of dye after regeneration. V (L) and V_r (L) are the volume of feed and regeneration emulsion.

In addition, the effect of co-existing ions on adsorptive performance was also investigated. The presence of heavy metals cationic ions (Pb^{2+} and Cd^{2+}) in dying effluents is often documented, and these cationic ions can create selectivity in the adsorptive removal of cationic CV dye. The dye sorption onto 3-MPA@PMNPs was investigated by varying initial co-existing cationic ions concentration of 1, 5, 25, 50, 100 and 1000 mg/L, respectively. 0.300 g/L of powered sorbent was mixed in a binary solution (50 mL) containing the heavy metals cationic ions (either Pb^{2+} or Cd^{2+}) and the CV dye (10 mg/L).

3 Results and Discussion

3.1 Characterization of 3-Marcaptopropanic Acid Functionalized Phytogenic Magnetic Nanoparticles

The comprehensive characterization of 3-MAP@PMNPs was formerly explained by Ali et al. [3,31]. Herein, only the important characteristics are described. The FTIR spectrum was studied to explore the nature of coating on the surface of prepared sorbent. The results revealed that the spectrum had a broad characteristic peak at around 3357–2962 cm^{-1}, which can be endorsed to –OH stretching vibrations. Importantly, thiol (–SH) characteristic peaks (at 2659 and 2511 cm^{-1}) and carboxylic (COOH) characteristic peak (at around 1633 cm^{-1}) suggested the smooth coating of 3-MPA ligand onto PMNPs, [23,32] as shown in Fig. 1I.

The powder XRD profiles of 3-MPA@PMNPs were obtained. The perceived reflections in the XRD profiles were suggested to belong to ferric oxide/hematite (Fe_2O_3), iron oxide/magnetite (Fe_3O_4), in addition to NaCl [33]. The XRD profile indicated peaks at $2\theta = 32.5°$, 35.2°, 45.4°, 57.3° and 62.8°, respectively (Fig. 1II). The peaks at $2\theta = 35.2°$

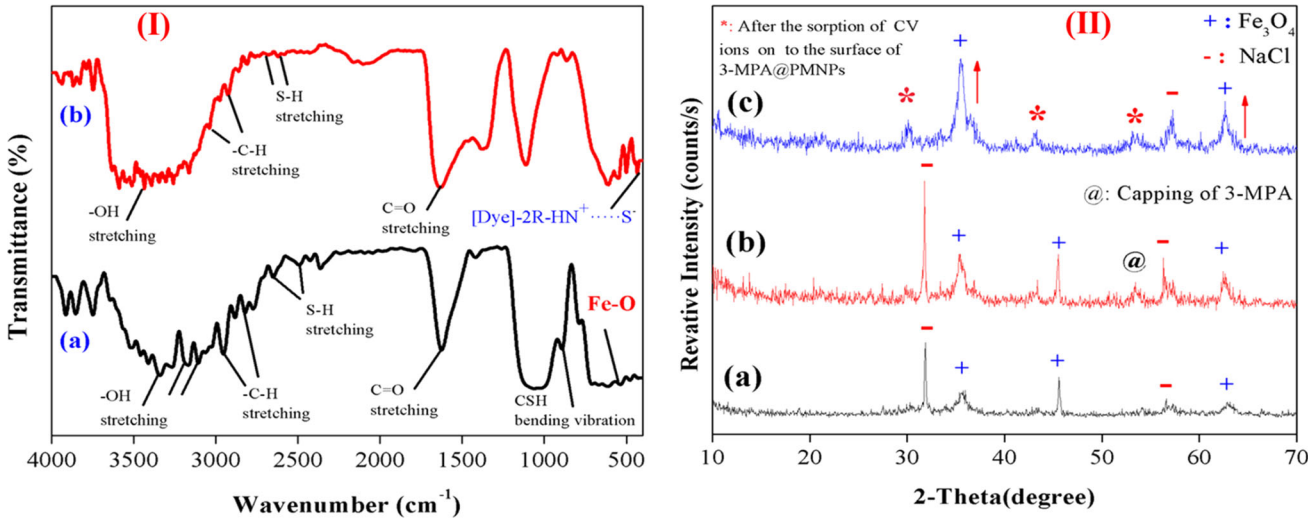

Fig. 1 **I** Fourier transforms infrared spectroscopic (FTIR) spectrum of: (**a**) 3-Marcaptopropanic acid functionalized phytogenic magnetic nanoparticles (3-MPA@PMNPs); (**b**) after sorption of crystal violet (CV) onto 3-MPA@PMNPs and **II** the powder XRD patterns of (**a**) phytogenic magnetic nanoparticles (PMNPs); (**b**) 3-MPA@PMNPs and (C) after the sorption of CV onto 3-MPA@PMNPs . (Reproduce from Ali et al. [31]—Published by The Royal Society of Chemistry, UK)

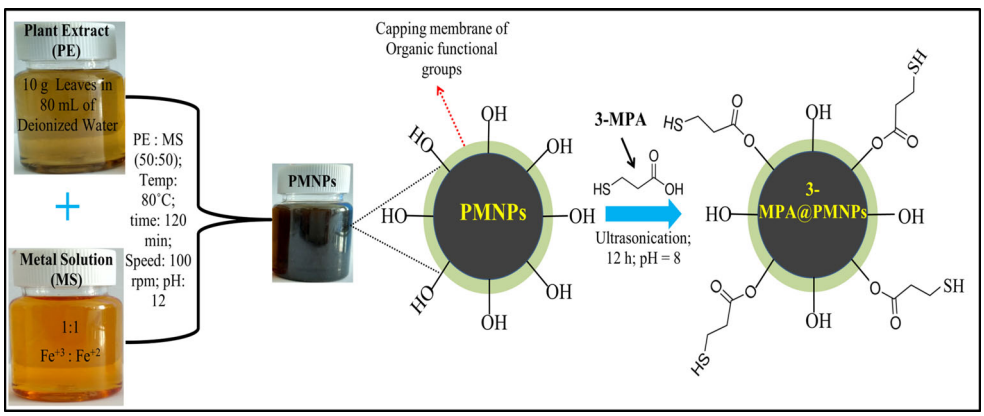

Fig. 2 Schematic of 3-Marcaptopropanic acid functionalized phytogenic magnetic nanoparticles (3-MPA@PMNPs) formation . (Reproduce from Ali et al. [3] with permission from Elsevier)

and 62.8° were principally showing the attendance of Fe_3O_4. These peaks can be linked to (220), (311), (400), (511) and (440) planes indexed of Fe_3O_4, as earlier registered in JCPD reference pattern 019-0629 [32,34]. Further, it was found that (–SH) functional group had bound with fabricated PMNPs. The characteristic peaks at $2\theta = 30°$ and $2\theta = 56°$, indicating the covering of (–SH) group onto PMNPs [35]. The formation scheme of the prepared sorbent is presented in Fig. 2.

Magnetic measurement results revealed that the values of remnant magnetization (M_r) and coercivity (H_c) are zero, suggesting the superparamagnetic nature of the sorbent (Fig. 3). The value of saturation magnetization (M_s) was 50.95 emu/g. The lower value of M_s compared to M_s (for bulk Fe_3O_4 = 93 emu/g) may be because of the occurrence of chemical reactions among capping agents and PMNPs [36–39]. In addition, Fig. 3 illustrated that 3-MPA@PMNPs can easily be separated from solution within 35 s by using magnet.

Based on the results obtained by TEM analysis, the manufactured particles were compact, fine, irregular in shape and monodisperse (Fig. 4a, b). Most of them are displaying cube shape structure and rests were indicating spherical in shape. On average, the diameter of the fabricated sorbents was 35–55 nm (Fig. 4). The surface of the 3-MPA@PMNPs was coated by organic matters from plant leafs extracts and 3-MPA ligands, which were acting influential role in restraining their aggregation and enhancing their dispersion and colloidal stability (Fig. 4a, b).

Similarly, as shown in Fig. 4c, spherical-shaped morphology was also noticed in SEM analysis with a size ranging from 30 to 50 nm [32,35].

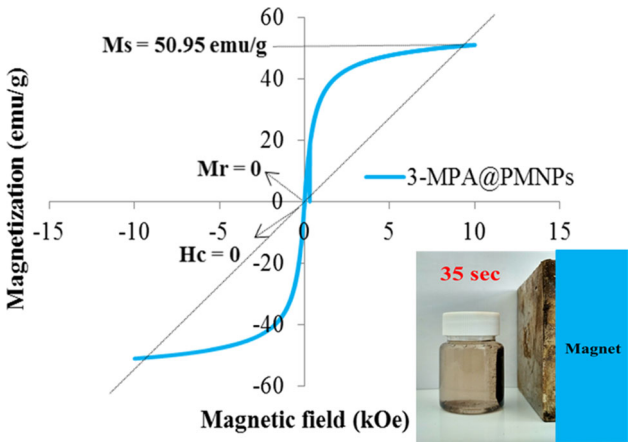

Fig. 3 M–H hysteresis loop/VSM measurement of 3-Marcaptopropanic acid functionalized phytogenic magnetic nanoparticles (3-MPA@PMNPs) at temperature 300 K, and inset photograph of magnetic separation study of 3-MPA@PMNPs using simple hand-held magnet (distance between the magnet and sample was 5 cm). (Reproduce from Ali et al. [3] with permission from Elsevier)

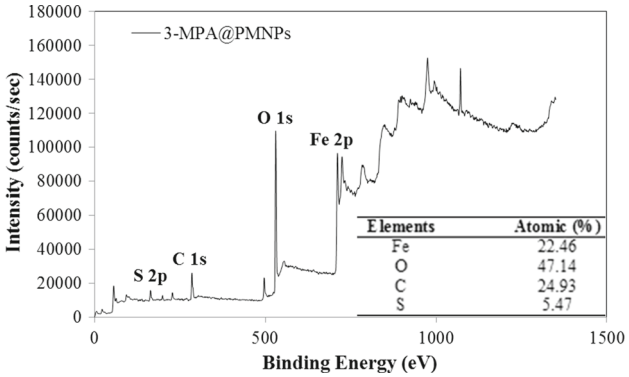

Fig. 5 X-ray photoelectron spectrum (XPS) of 3-Marcaptopropanic acid functionalized phytogenic magnetic nanoparticles (3-MPA@PMNPs) (inset table is the atomic percentages of the elements). (Reproduce from Ali et al. [31]—Published by The Royal Society of Chemistry, UK)

Moreover, the XPS profile depicted three (03) main peaks at around 710.58/724.6, 529.95, and 284.79 eV, corresponding to Fe $2p$, O $1s$ and C $1s$, respectively (Fig. 5). Importantly, a minor peak developed at around 163.5 eV for S $2p$, hinting the topping of 3-MPA ligand on PMNPs (Fig. 6d). Further, the high-resolution XPS spectra were also obtained to check the structure of iron oxide (Fig. 6a–d). As shown in Fig. 6a, two main peaks were developed (at around 710.58 and 724.6 ev) from 700 to 740 eV, which were associated to Fe $2p_{3/2}$ and Fe $2p_{1/2}$, respectively, evidencing the occurrence of Fe_3O_4. The binding energy resembling to Fe $2p_{3/2}$

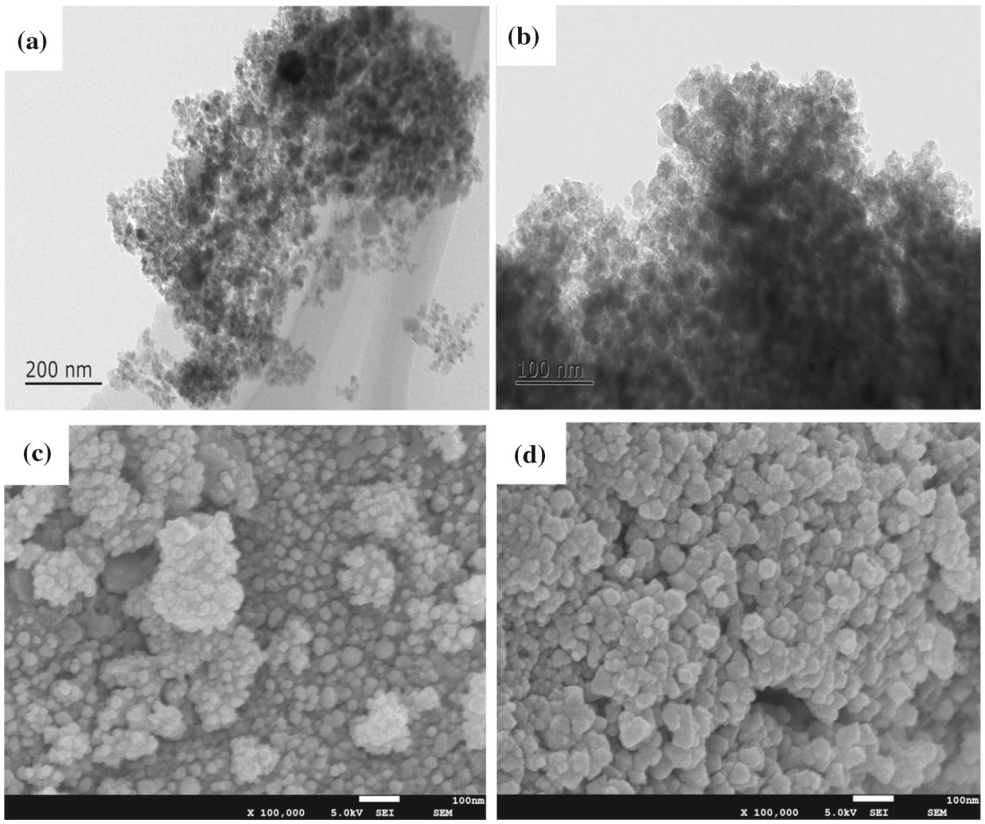

Fig. 4 Transmission electron microscopic (TEM) images of 3-Marcaptopropanic acid functionalized phytogenic magnetic nanoparticles (3-MPA@PMNPs). **a** 200 nm scale bar; **b** 100 nm scale bar, and SEM images of 3-MPA@PMNPs **c** before and **d** after sorption of crystal violet (CV) dye . (Reproduce from Ali et al. [31]—Published by The Royal Society of Chemistry, UK)

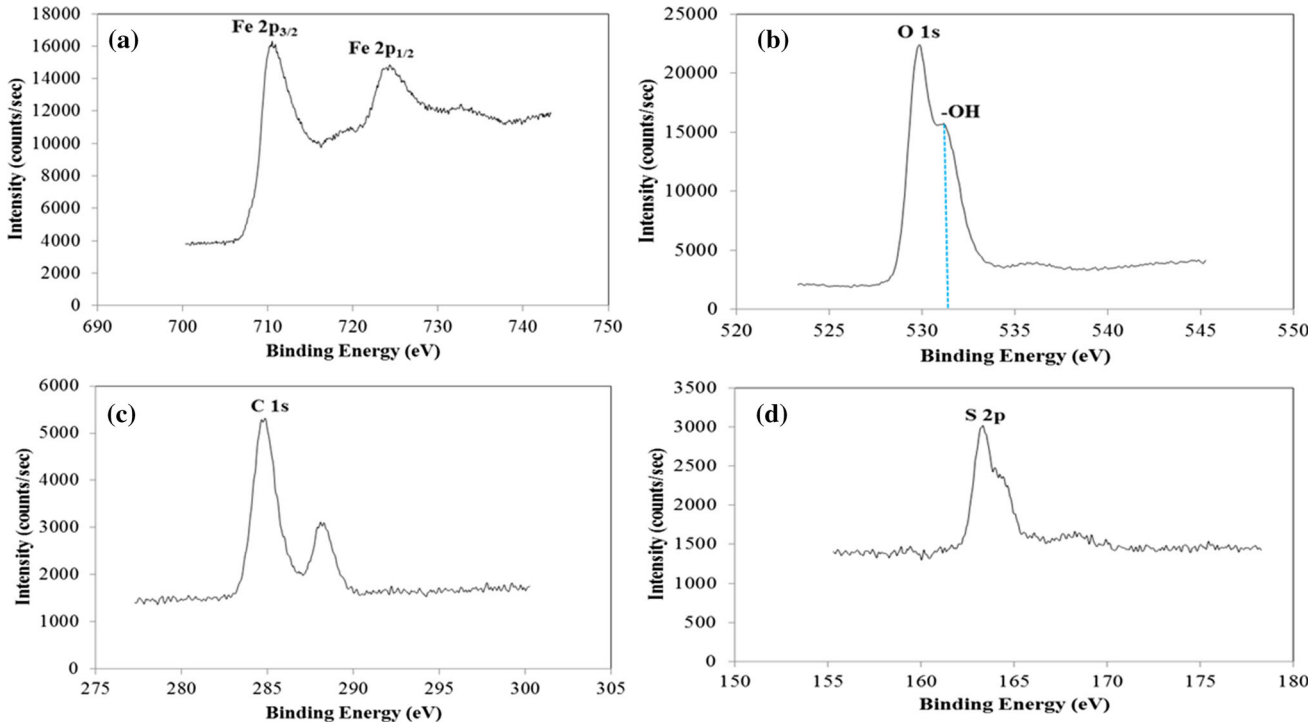

Fig. 6 **a** High-resolution X-rays photoelectron spectra (XPS) of Fe 2*p*; **b** high-resolution XPS spectra of O 1*s*; **c** high-resolution XPS spectra of C 1*s*; **d** high-resolution XPS spectra of S 1*s* . (Reproduce from Ali et al. [31]—Published by The Royal Society of Chemistry, UK)

is typical for Fe in iron oxide/ Fe_3O_4. A major peak developed at around 529.95 eV, which might be ascribed to the bonding of O atoms with iron (Fe–O). In contrast, a minor peak at around 532.8 eV might be assigned to the oxygen atom in the hydroxyl/–OH functional groups (Fig. 6b). Moreover, C 1*s* spectra showed two peaks at 285.7 and 287.6 eV in the range of 275–305 eV (Fig. 6c). These features indicated the presence of two C atom with different chemical nature. The peak at 285.7 eV can be linked to alcoholic (C–O) and/or polyphenolic (O–H) groups.

Furthermore, N_2 adsorption–desorption results depicted that the hysteresis loop of the prepared material was associated to type IV isotherm model and its hysteresis loop was very close with H4-type, as categorized by IUPC. The specific surface area was found to be 115.42 m^2/g, as estimated by BET method (Fig. 7). Interestingly, the obtained specific surface area was higher than most of the documented green magnetic NPs [6–8,20–24,40,41]. Barrett–Joyner–Halenda (BJH) model was used to calculate average pore size and total pores volume. The average pore radius of the material was acquired to be 17.052 nm (Fig. 7), while the total pores volume was 0.238 cm^3/g, suggesting the existence of a mesoporous structure of the material. Hence, the fabricated material shows the availability of mesoporosity, which may help diffusion of contaminants via pores.

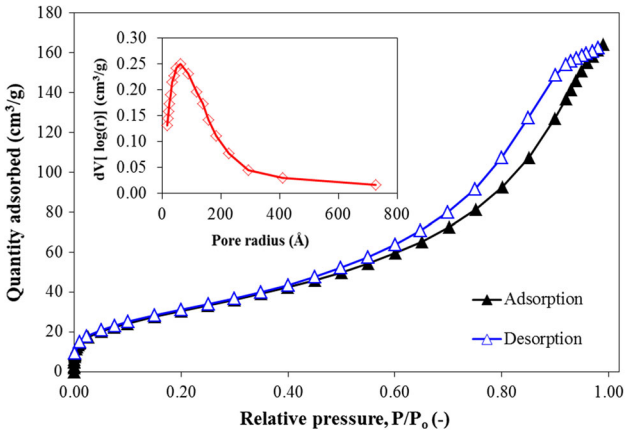

Fig. 7 N_2 adsorption–desorption isotherm at (77 K). Pore size distribution (inset) of 3-Marcaptopropanic acid functionalized phytogenic magnetic nanoparticles (3-MPA@PMNPs) . (Reproduce from Ali et al. [3] with permission from Elsevier)

3.2 Adsorption Properties of 3-Marcaptopropanic Acid Functionalized Phytogenic Magnetic Nanoparticles (3-MPA@PMNPs) for the Removal of the Crystal Violet (CV) Dye

3.3 Influence of Adsorbent Dose

To investigate the optimal quantity of adsorbent for enhancing the interfaces between CV ions with the adsorption sites

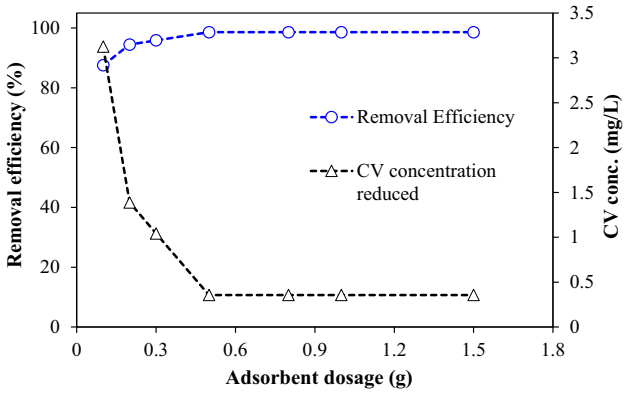

Fig. 8 Effect of adsorbent dosage on the removal of crystal violet (CV) dye by 3-Marcaptopropanic acid functionalized phytogenic magnetic nanoparticles (3-MPA@PMNPs) (dosages = 0.1 − 1.5 g/L; Co = 25 mg/L; contact time = 24 h)

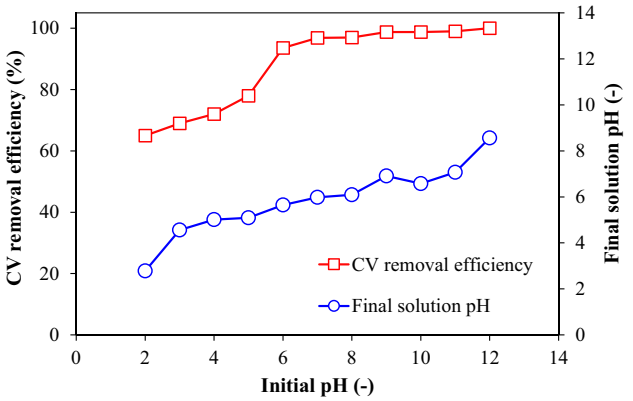

Fig. 9 Effect of solution pH on the removal efficiency of crystal violet (CV) onto 3-Marcaptopropanic acid functionalized phytogenic magnetic nanoparticles (3-MPA@PMNPs), interval of pH (2–12), initial dye concentration: 25 mg/L. dosage: 0.5 g/L; solution volume: 50 mL; temperature: 25 °C and agitation time: 120 min

of adsorbent, different amount of 3-MPA@PMNPs dosages (0.1–1.5 g/L) were mixed in dye solution (25 mg/L) for 24 h. The findings indicated that a maximum of 87.5% removal efficiency was achieved at the lowest adsorbent dosage; subsequently, the removal efficiency was increased from 87.5 to 98.57% by increasing dosages from 0.1 to 0.5 g/L and later it was almost stable (Fig. 8). This might be due to the increase in the presence of higher amount of free/active sites on the adsorbents with the increase in adsorbent dosages, whereas after the dose of 0.50 g/L, the removal performance was constant, suggesting the equilibrium among CV molecules and adsorbents. Hence, 0.5 g/L of adsorbent dosage was selected for further studies.

3.3.1 Effect of Solution pH on Sorption

The effect of solution pH on sorption of CV was investigated by varying pH from 2 to 12. Initially, the removal efficiency was slowly increased from 65 to 93.57% in the range of pH 2–6 and then increased from 93.57 to 98.75% in the pH range of 6–10. Thereafter it was reached up to 100% in the range of pH 11–12 (Fig. 9). The sorption of cationic CV was mainly associated with the surface charge on the adsorbent, which could influence by the variation of solution pH. This might be because the pH_{PZC} of the prepared material was 5.19 (Fig. SI), thus, the surface of the adsorbent was negatively charged at pH >. $pH_{PZC,}$ which endorsed the sorption of CV cationic ions onto adsorbent surface, while at lesser pH, when pH < .pH_{PZC} the adsorbent surface was positively charged, thereby boosting electrostatic repulsion among cationic of CV molecules and the co-existed surplus protons/H^+ ions. Meanwhile, the positively charged adsorbent surface inhibited the sorption of CV ions. Hence, above pH 5.19, the CV removal efficiency was increased from 59 to 98.57% because

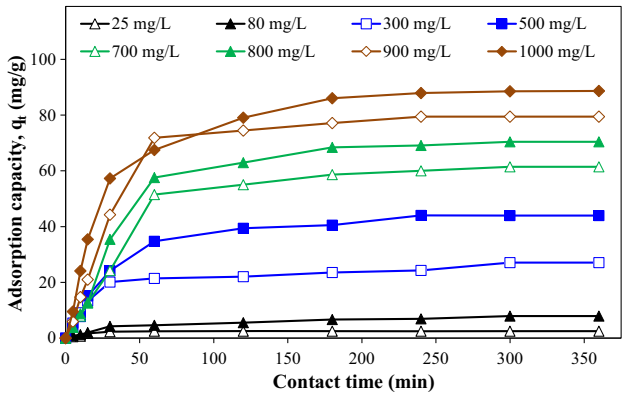

Fig. 10 Kinetics of crystal violet (CV) dye sorption onto 3-Marcaptopropanic acid functionalized phytogenic magnetic nanoparticles (3-MPA@PMNPs) (dosage = 0.5 g/L)

pH > .pH_{PZC}, while below pH 5.19, CV removal efficiency was low due to the repulsion among cations.

3.3.2 Kinetics of Dye (CV) Sorption onto 3-Marcaptopropanic Acid Functionalized Phytogenic Magnetic Nanoparticles (3-MPA@PMNPs)

The effect of contact time on the removal of CV dye by 3-MPA@MPA was noticed using a fixed amount of adsorbents (0.500 g/L) at different initial concentrations of CV dye (25–1000 mg/L). As it can be noticed in Fig. 10, that firstly the adsorption capacity of CV was sharply increased and then reached plateau. The rapid adsorption of CV dye at different concentration might be associated to the accessibility of a substantial amount of free/active sites for fresh 3-MPA@PMNPs and then slowly decreases. This decrease of CV dye sorption might be due to the sluggish pore diffusion of CV ions into the bulk of 3-MPA@PMNPs. On

Table 1 Kinetic parameters for the adsorption of crystal violet (CV) onto 3-Marcaptopropanic acid functionalized phytogenic magnetic nanoparticles at different initial concentration of CV

Co (mg/L)	q_e (exp.) (mg/g)	Pseudo-first-order kinetic model			Pseudo-second-order kinetic model			Elovich kinetic model			Intraparticle diffusion/Webber and Morris kinetic model			Liquid film diffusion kinetic model		
		$\log(q_e - q_t) = \log q_e - \frac{tk_1}{2.303}$			$\frac{t}{q_t} = \frac{1}{h} + \frac{t}{q_e}$			$q_t = \frac{1}{\beta \ln \alpha\beta} + \frac{1}{\beta \ln t}$			$q_t = k_{ipd} t^{0.5}$			$\ln(1-F) = -k_{fd}t$		
		K_1 (min^{-1})	R^2		K_2 (min^{-1})	h (mg g^{-1} min^{-1})	R^2	α (mg g^{-1} min^{-1})	β (g/mg)	R^2	K_{ipd} (mg g^{-1} min$^{-0.5}$)	I	R^2	K_{fd} (g/mg)	I	R^2
25	2.46	−0.0019	0.03		0.39	0.49	0.99	0.49	0.46	0.86	1.10	0.77	0.64	−0.045	−2.42	0.008
80	7.88	−0.0027	0.88		0.11	1.57	0.97	1.57	1.48	0.95	3.52	0.48	0.94	−0.021	−0.54	0.031
300	27.09	−0.0036	0.90		0.03	5.41	0.99	5.41	4.72	0.96	12.11	6.20	0.82	−0.044	−0.90	0.001
500	43.93	−0.005	0.92		0.02	8.78	0.98	8.78	8.88	0.95	19.65	4.88	0.87	−0.019	−0.78	0.0051
700	61.46	−0.0055	0.92		0.01	12.29	0.96	12.29	13.00	0.91	27.48	3.02	0.87	−0.013	−0.77	0.056
800	70.41	−0.0058	0.92		0.07	14.08	0.94	14.08	14.99	0.91	31.49	3.88	0.86	−0.011	−0.80	0.061
900	79.47	−0.0059	0.88		0.01	15.89	0.97	15.89	16.63	0.92	35.54	8.70	0.83	−0.015	−0.95	0.001
1000	88.65	−0.0072	0.88		0.01	17.73	0.99	17.73	17.39	0.96	39.64	14.01	0.86	−0.022	−0.66	0.34

Given in supplementary information (Text-SIV)

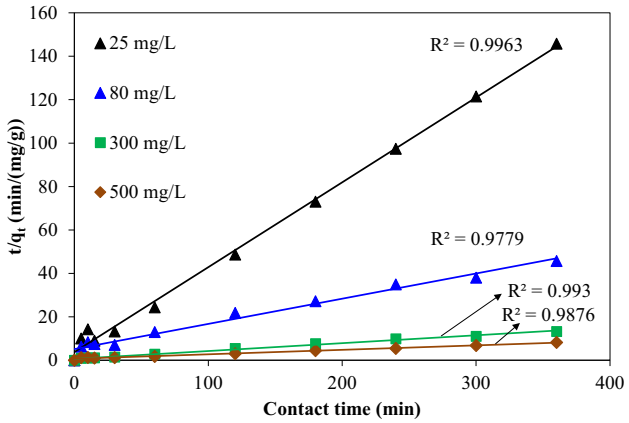

Fig. 11 The linear plot of pseudo-second-order model of crystal violet (CV) dye sorption onto 3-Marcaptopropanic acid functionalized phytogenic magnetic nanoparticles (3-MPA@PMNPs) (dosage = 0.5 g/L)

average, 88.65 mg/g of adsorptive capacity was achieved at equilibrium (120 min), while rapid adsorption rate was noticed within 60 min along-with 98.57% of dye removal efficiency. Moreover, sorption mechanism was also explored via estimating kinetic parameters. Various types of kinetics models (as details given in Text-SIII) were utilized to fix the experimental data. The findings of these models are enlisted in Table 1

As shown in Fig. 11 and Table 1, it can be suggested that sorption of CV dye onto/by the sorbent can effectively be expressed by pseudo-second-order kinetic model because its regression coefficient ($R^2 = 0.99$) values were higher than other models, hinting the presence of ion-exchange and/or chemisorption mechanism [6]. Moreover, as shown in Fig. 12, Weber and Morris kinetic model was employed to assess the diffusion mechanism, and it can be noticed that the curves can be subdivided into multi-linear plots which indicated that more than one process (like boundary layer adsorption) might be convoluted in the adsorption of CV ions by the prepared sorbent (Fig. 12). Despite the R^2 values indicated non-applicability of this model (Table 1). For instance, initially, fast adsorption of cationic CV ions is indicating the existence of large amount of fresh/free sites onto adsorbent surface. Similarly, k_{ipd} values are also growing with the enhancement of CV dye concentration in the solution which indicating that firstly CV ions occupied exterior vacant sites and then these ions pursue to enter into the pores of the adsorbents. That's why initially sorption capacity was high then subsequently slowed down gradually to reach equilibrium. On the other hand, the values of intercept were also increased and indicated the boundary layer diffusion effect because of the CV molecules entered into the pores of 3-MPA@PMNPs. Consequently, it might be stated that CV ions sorption onto 3-MPA@PMNPs was convoluted because of the presence

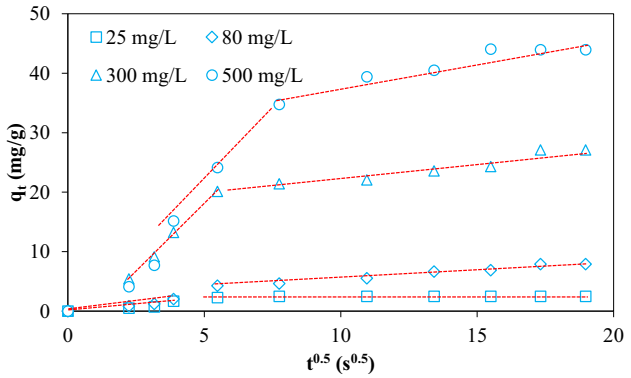

Fig. 12 Intra-particle diffusion kinetic model fit for the crystal violet (CV) dye sorption onto 3-Marcaptopropanic acid functionalized phytogenic magnetic nanoparticles (3-MPA@PMNPs) (dosage = 0.5 g/L)

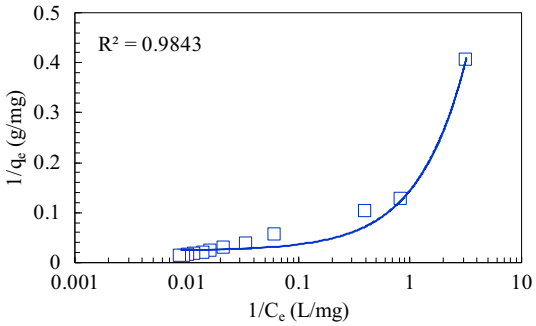

Fig. 13 The linear plot of Langmuir isotherm model for crystal violet (CV) dye sorption onto 3-Marcaptopropanic acid functionalized phytogenic magnetic nanoparticles (3-MPA@PMNPs) (dosage = 0.5 g/L)

of both the surface adsorption (chemisorption/ion-exchange mechanism) and boundary layer adsorption.

3.3.3 Sorption Isotherm Study

Adsorption isotherm results revealed that Langmuir model presented the excellent fit. As shown in Fig. 13 and Table 2, the value of R^2 (for Langmuir model) was greater than other isotherm models. On the other hand, the value of K_L for CV was in the range of 0.28–0.99, suggesting that adsorption was favorable. The results hinted the monolayer sorption of dye onto homogenous sites of the prepared sorbent. The calculated maximum sorptive capacity was 88.65 mg/g (Table 2).

3.3.4 Thermodynamic Studies

The values of ΔG^o were negative at all reaction temperatures, suggesting the thermodynamically feasible spontaneous nature of CV adsorption by 3-MPA@PMNPs (Table 3). The negative value of enthalpy of sorption (ΔH^o) hinted the exothermic nature of adsorption in the temperature of 298.15–333.15 K. This value was greater 20.9 KJ/mole, suggested the chemisorption and/or ion-exchange mechanism, as previously ensured by isotherm and kinetic studies. In addition, the negative value of entropy (ΔS^o) hinted a decrease in uncertainty/adsorbed species degree of freedom at the solid-solution boundary during adsorption process. A slight increase in adsorptive capacity (from 2.46 to 2.48 mg/g) was also detected with the increase in reaction temperature from 298.15 to 333.15 K, though CV removal efficiency was constant (Fig. 14). This can be assigned due to the formation of fresh/or free spots onto sorbent or the increased rate of pore diffusion.

3.3.5 Proposed Removal Mechanism

For exploring removal mechanism, the FTIR, XRD and SEM analyses were also carried out after the sorption of CV by the prepared sorbent, in addition to isotherm, kinetics and thermodynamic studies. The FTIR results showed that two important peaks at around 2659 and 2511 cm^{-1} shifted to 2632 and 2501 cm^{-1}, hinting the attachment of cations onto sorbent. Further, the characteristic peak at around 435 cm^{-1} was arose, suggesting the bonding between S–H and cationic ions of CV (e.g., [Dye]-2$RN^+ \cdots\cdots S^-$). The stretching vibrations of C–H (related to methyl groups) were also reduced, indicating the sorption of CV molecules onto sorbent (Fig. 1b). This might be due to the presence of hydrophobic interaction between CH_3 and CH_3. Similarly, the stretching vibration of (–OH) functional groups were also altered and reduced, indicating the sorption of CV molecules with O–H via electrostatic interactions (e.g., [Dye]-2$RN^+ \cdots\cdots O^-$). Thus, FTIR results confirmed the sorption of CV ions onto sorbent via connection between S–H and O–H functional groups (Fig. 1b). On the other hand, the intensity of characteristic peaks at $2\theta = 30°$, $2\theta = 35.2°$, $2\theta = 56°$ and $2\theta = 62°$ was also slightly affected, indicating the sorption of CV molecules onto sorbent. Moreover, a new peak also appeared at $2\theta = 44°$; it may due to the sorption of CV molecules (Fig. 1II). The granular size was improved after the sorption of CV molecules (Fig. 44). This increase in size might be due to the attachment of CV molecules, while the morphology of 3-MPA@PMNPs was almost stable after the sorption of CV molecules indicated the high stability of 3-MPA@PMNPs. Moreover, the evidence attained from the isotherm, kinetic and thermodynamic investigations along with the verity that CV dye and functional groups onto sorbent are oppositely charged, directing the ion exchange might be the principal sorptive mechanism. In solution, the cationic ions of CV dye mainly attached with (–OH) groups due to electrostatic interaction. However, the development of chelate can also be occurred due to the attachment of cations with (–SH) functional groups. In addition to electrostatic interaction, hydrophobic interaction might be happened owing to the presence of hydrophobic functional groups (R = CH_3) in CV dye molecules.

Table 2 Isotherm constants for adsorption of crystal violet (CV) onto 3-Marcaptopropanic acid functionalized phytogenic magnetic nanoparticles (3-MPA@PMNPs)

Isotherm models	Equations	Parameters	Values
Langmuir isotherm model	$\frac{1}{q_e} = \frac{1}{K_L q_{max} C_e} + \frac{1}{q_{max}}$	q_{max} (mg/L)	88.65
	$K_L = \frac{1}{1+bC_e}$	b (L/mg)	0.022
		K_L	0.28–0.99
		R^2	0.981
Freundlich Isotherm model	$\log q_e = \left(\frac{1}{n}\right) \log C_e + \log k_F$	$1/n$	0.6357
		K_f (mg/L)	0.5584
		R^2	0.893
Temkin isotherm model	$q_e = \left(\frac{RT}{B_T}\right) \log C_e + \left(\frac{RT}{B_T}\right) \log K_T$	K_T (L/g)	2.0394
		B_T (KJ/mol)	29.623
		R^2	0.780
Dubinin–Radushkevich isotherm model	$\ln q_e = \ln q_m - \beta\varepsilon^2$	q_{max} (mg/L)	88.65979381
		E (KJ/mol)	0.383488134
		β (mol^2/J^2)	3.3999
		R^2	0.273

Given in supplementary information (Text-SV)

Table 3 Thermodynamic parameters values for the adsorption of crystal violet (CV) onto 3-Marcaptopropanic acid functionalized phytogenic magnetic nanoparticles (3-MPA@PMNPs) at various reaction temperatures (K)

Thermodynamic equations	Temperature (K)	ΔG^o (KJ/mol)	ΔH^o (KJ/mol)	ΔS^o (KJ/mol K)
$\Delta G^\circ = -RT \ln K_D$	298.15	−5123.378885	−47.44	−8.67
	303.15	−5313.461504		
$\ln K_D = \frac{\Delta S^\circ}{R} - \frac{\Delta H^\circ}{RT}$	313	−6216.234409		
	323.15	−6764.217316		
	333.15	−8548.978774		

Given in supplementary information (Text-SVI)

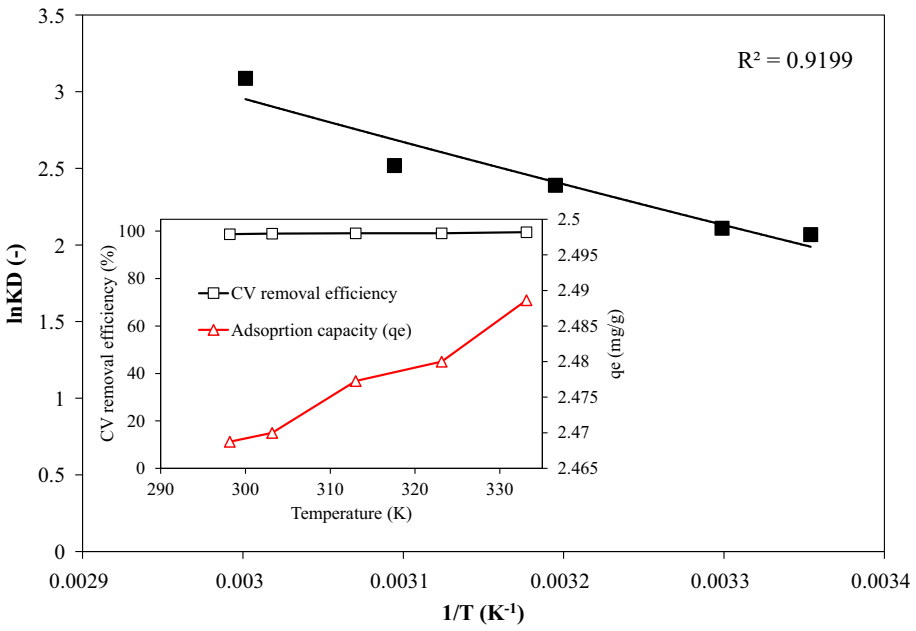

Fig. 14 Thermodynamic plot for the sorption of crystal violet (CV) dye sorption onto 3-Marcaptopropanic acid functionalized phytogenic magnetic nanoparticles (3-MPA@PMNPs) (dosage = 0.5 g/L, Co = 25 mg/L); inset graph is the effect of temperature on the adsorptive removal and capacity of CV dye

Moreover, before treatment, UV–vis spectra showed major peaks at 240, 292, and 577 nm (Fig. 15). Then, initially major peaks were reduced rapidly within the contact time 15 min. While subsequently decreased approximately in proportion to each other within the contact time of 120 min and then almost disappeared at the stage of equilibrium (Fig. 15). This indicates that initially sorption rate was high due the availability of a large amount of vacant/free sites onto sorbent [8]. This change in peaks indicated that CV molecules were significantly adsorbed onto sorbent. Similar findings were reported by various researchers [42,43].

3.3.6 Stability and Reusability of 3-Marcaptopropanic Acid Functionalized Phytogenic Magnetic Nanoparticles

The prepared sorbent sustained its working up to five (05) cycles then steadily reduced (Fig. 16). Importantly, the etching/ dissolution of iron or disintegration of adsorbent were not notice during the first five (05) treatment cycles. This hints that there was no disrobing of 3-MPA coated PMNPs happened. However, after five (05) treatment cycles, the reusability was significantly declined owing to the destruction of adsorbent caused by the leakage/etching of Fe^{o}. Overall, the coating of 3-MPA was stable and material persisted > 85% sorption–desorption efficiency up to five treatment cycles.

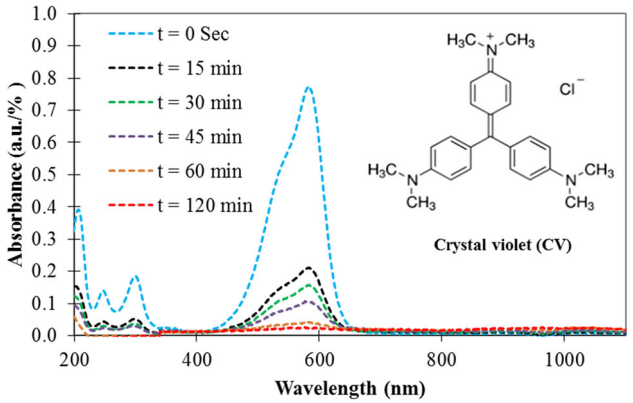

Fig. 15 Study of adsorptive removal of crystal violet (CV) via UV–vis spectra; [inset figures shows chemical structure of CV dye] (adsorbents dosage = 0.5 g/L)

3.3.7 Influence of co-present constituents

For investigating the sorption selectivity, a binary system (cationic metals ions + cationic CV dye) was prepared and used. The co-presence of cationic ions did not influence on the sorptive removal of cationic CV using 3-MPA@PMNPs under all the experimented concentrations (Fig. 17). However, the presence of higher concentration of cadmium (Cd^{2+}) in solutions inhibited the CV sorption using 3-MPA@PMNPs. A higher selectivity was noticed in the presence of lead (Pb^{2+}) than Cd^{2+} within the contact time of 24 h, while initially (within the contact time of 1 h), both metals ions inhibited adsorptive removal of CV using 3-MPA@PMNPs (Fig. SII). This suggests that a competition was developed among the excess cationic CV ions and the CV ions adsorbed onto 3-MPA@PMNPs. Cd^{2+} ions restrained the adsorption to a larger extent than Pb^{2+}. It might be due to the formation of inner-sphere complex by the reaction between metal ions and adsorbent. In addition, the hydrated radii of Pb^{2+} (4.01 Å) are lower than Cd^{2+} (4.26 Å), and it can also influence on the adsorptive removal of other cations onto 3-MPA@PMNPs. It can also be addressed in this way that Pb^{2+} and Cd^{2+} selectivity might be owing to attendance of mercapto/(–SH) group onto sorbent and the (–SH) group was playing governing job in the choosiness of Pb^{2+} and Cd^{2+} owing to softness of the base because the interaction between

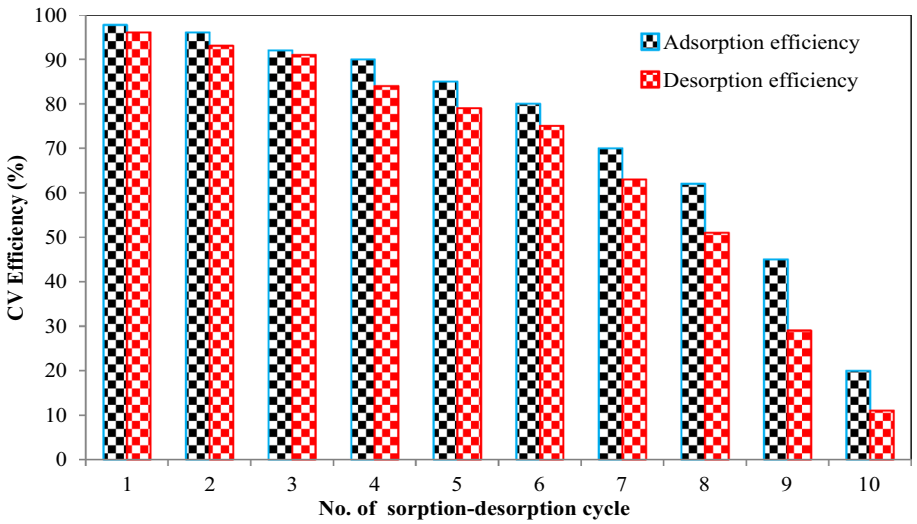

Fig. 16 Stability and reusability of 3-Marcaptopropanic acid functionalized phytogenic magnetic nanoparticles (3-MPA@PMNPs) for consecutive sorption–desorption cycles (20 mL of 0.1MEDTA regeneration solution; adsorbents dosage = 0.5 g/L, CV initial concentration (C_o) = 25 mg/L)

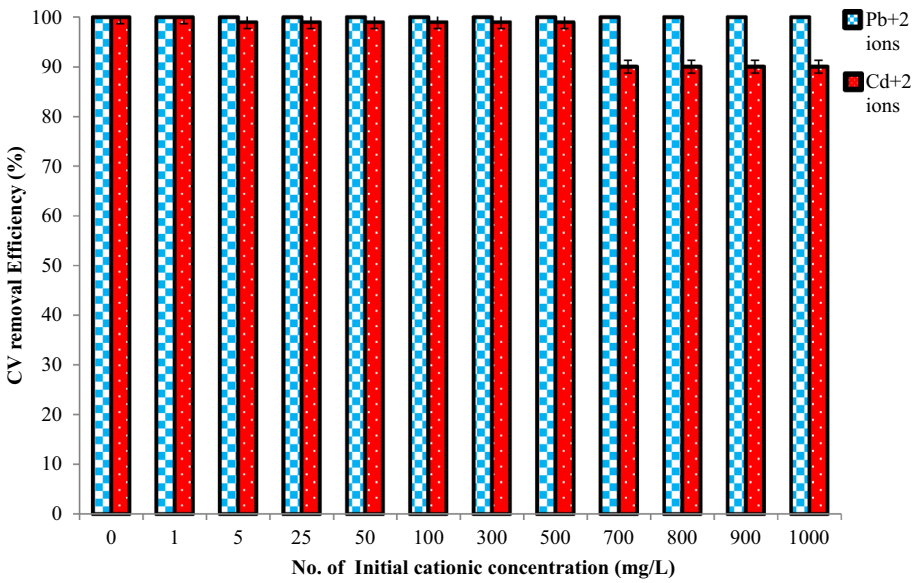

Fig. 17 Influence of co-present cationic ions on crystal violet (CV) removal by 3-Marcaptopropanic acid functionalized phytogenic magnetic nanoparticles (3-MPA@PMNPs) (adsorbents dosage = 0.3 g/L; CV initial concentration (C_o) = 10 mg/L; contact time: 24 h)

Table 4 Comparison of 3-Marcaptopropanic acid functionalized phytogenic magnetic nanoparticles (3-MPA@PMNPs) with other sorbents for the sorption of cationic crystal violet (CV) dyes

Cationic dye	Sorbents	q_e (mg/g)	Reusability	References
CV	Bottomash	12.66	–	[44]
CV	Bottomash	13.06	–	[45]
CV	Orange peel	14.30	–	[46]
CV	Jute fiber carbon	27.99	–	[47]
CV	Coniferous pinus bark powder (CPBP)	32.78	–	[48]
CV	Acacia niloticaleaves	33.00	–	[49]
CV	*Artocarpus heterophyllus* (jackfruit) leaf powder (JLP)	43.39	–	[50]
CV	NaOH-modified rice husk (NMRH)	44.87	–	[51]
CV	Spherical mesoporous silica (meso-silica MCM-41)	46.20	–	[52]
CV	*Punica granatum* shell	50.21	–	[53]
CV	AC (Waste apricot)	52.86	–	[54]
CV	Nano composite CuO/MCM-41	52.90	–	[52]
CV	*Yarrowiali polytica* ISF7	59.40	–	[55]
CV	Rice husk	64.87	–	[56]
CV	Treated ginger waste (TGW)	64.93	–	[57]
CV	Peanute shells	76.40	–	[58]
CV	Palmkernelfiber	78.90	–	[59]
CV	Ag nanoparticles (AgNPLs) chemically immobilized onto activated carbon (ACAgNPLs)	87.20	–	[60]
CV	**3-MPA@PMNPs**	**88.65**	**Yes**	**P.S**
CV	Opal	101.13	Yes	[61]

q_e, sorption capacity (mg/g); P.S, present study; –, not reported

soft acid and soft base is predominate [3], while mercapto (–SH) group is a soft base and preferably desire to interact with soft acid (i.e., metal ions) then subsequently the formation of chelate could happen via chelation mechanism due to the presence of S atom ligand onto sorbent [20–24]. In addition, CV is a basic cationic dye and it selectivity may inhibit in the presence of soft acid (metal ions) and (–SH) group onto 3-MPA@PMNPs. However, the conclusions illustrated that CV adsorption was inhibited initially but later with the increase of contact time, adsorptive removal was acceler-

ated. This indicates that 3-MPA@PMNPs had enough active/ vacant sites for the sorption of a greater amount of cationic ions. Therefore, the pre-knowledge of the co-presence of different cationic ions is mandatory to compatibly optimize the operational prerequisites for smooth application of 3-MPA@PMNPs because the influence of co-existing ions could be varied for different cationic days.

3.4 Comparison of 3-Marcaptopropanic Acid Functionalized Phytogenic Magnetic Nanoparticles (3-MPA@PMNPs) with Other Sorbents

Lastly, the prepared material had superior characteristics than other reported sorbents in term of sorption capacity, kinetics, reusability, magnetic separation and green fabrication (Table 4). These features make 3MPA@PMNPs a prerequisite/ desirable alternative green material/adsorbent to eliminate cations from many fields.

4 Conclusions

An environment-friendly, non-toxic, cost-effective, biocompatible green recipe was utilized to manufacture phytogenic magnetic nanoparticle (PMNPs), and their surfaces were successfully functionalized by 3-mercaptopropionic acid (3-MPA), as ensured through various instrumentations including FTIR, SEM, BET, powder XRD, TEM and VSM techniques. Further, the adsorptive performance of functionalized 3-MPA@PMNPs was also investigated using a toxic cationic CV dye. The 3-MPA@PMNPs presented a high sorption rate (98.57% CV dye removal within 120 min). The experimental data matched appropriately with Langmuir isotherm model and pseudo-second-order kinetics model, hinted that monolayer sorption of CV dye by 3-MPA@PMNPs via ion-exchange and/or chemisorption mechanism. The fabricated adsorbent depicted comparable sorption capacity of 88.65 mg/g at 25 °C. Similarly, thermodynamic study demonstrated that adsorption was favorable, exothermic and spontaneous. Moreover, the findings obtained by FTIR and XRD analysis indicated that cationic CV dye adsorbed owing to the manifestation of electrostatic interaction and the development of chelate or chelation with (–OH) functional groups and (–SH) thiol ligand affixed on the surface of 3-MPA@PMNPs. in addition, the prepared sorbent can quickly be separated from solution within 35 s using magnet owing to their superparamagnetic nature. The recovered material reused for at-least five (05) times and maintained removal efficiency above 85%. Overall, the prepared sorbent is depicting a comparable high adsorptive efficiency, and its kinetics shows a good future for its applications in water/ wastewater treatment process ([62,63].

Acknowledgements This work was supported by the State Key Laboratory of Environmental Criteria and Risk Assessment (No. SKLECRA 2013FP12) and Shandong Province Key Research and Development Program (2016GSF115040). The first author would like to thanks for the financial support by the Chinese Scholarship Council, China (CSC No: 2016GXYO20).

Compliance with Ethical Standards

Conflict of interest The authors declare that they have no conflict of interest.

References

1. Ali, I.; Peng, C.; Naz, I.; Khan, Z.M.; Sultan, M.; Islam, T.; Abbasi, I.A.: Phytogenic magnetic nanoparticles for wastewater treatment: a review. RSC Adv. **2017**(7), 40158–40178 (2017a)
2. Ali, I.; Peng, C.; Khan, Z.M.; Naz, I.: Yield cultivation of magnetotactic bacteria and magnetosomes: a review. J. Basic Microbiol. **57**(8), 643–652 (2017b)
3. Ali, I.; Peng, C.; Naz, I.: Removal of lead and cadmium ions by single and binary systems using phytogenic magnetic nanoparticles functionalized by 3-marcaptopropanic acid. Chin. J. Chem. Eng. (2018a). https://doi.org/10.1016/j.cjche.2018.03.018
4. Vakili, M.; Rafatullah, M.; Salamatinia, B.; Abdullah, A.Z.; Ibrahim, M.H.; Tan, K.B.; Gholami, Z.; et al.: Application of chitosan and its derivatives as adsorbents for dye removal from water and wastewater: a review. Carbohydr. Polym. **113**, 115–130 (2014)
5. Yagub, M.T.; Sen, T.K.; Afroze, S.; Ang, H.M.: Dye and its removal from aqueous solution by adsorption: a review. Adv. Colloid Interface Sci. **209**, 172–184 (2014)
6. Cheera, P.; Karlapudi, S.; Sellola, G.; Ponneri, V.: A facile green synthesis of spherical Fe_3O_4 magnetic nanoparticles and their effect on degradation of methylene blue in aqueous solution. J. Mol. Liq. **221**, 993–998 (2016)
7. Weng, X.; Huang, L.; Chen, Z.; Megharaj, M.; Naidu, R.: Synthesis of iron-based nanoparticles by green tea extract and their degradation of malachite. Ind. Crops Prod. **51**, 342–347 (2013)
8. Abbassi, R.; Yadav, A.K.; Kumar, N.; Huang, S.; Jaffe, P.R.: Modeling and optimization of dye removal using "green" clay supported iron nano-particles. Ecol. Eng. **61**, 366–370 (2013)
9. Sivaraj, R.; Namasivayam, C.; Kadirvelu, K.: Orange peel as an adsorbent in the removal of acid violet 17 (acid dye) from aqueous solutions. Waste Manag. **21**, 105–110 (2001)
10. Lakshmi, U.R.; Srivastava, V.C.; Mall, I.D.; Lataye, D.H.: Rice husk ash as an effective adsorbent: evaluation of adsorptive characteristics for Indigo Carmine dye. J. Environ. Manag. **90**, 710–720 (2009)
11. Gong, R.; Ding, Y.; Li, M.; Yang, C.; Liu, H.; Sun, Y.: Utilization of powdered peanut hull as biosorbent for removal of anionic dyes from aqueous solution. Dyes Pigments **64**(3), 187–192 (2005)
12. Namasivayam, C.; Kumar, M.D.; Selvi, K.; Begum, R.A.; Vanathi, T.; Yamuna, R.T.: 'Waste'coir pith—a potential biomass for the treatment of dyeing wastewaters. Biomass Bioenergy **21**(6), 477–483 (2001)
13. Porkodi, K.; Kumar, K.V.: Equilibrium, kinetics and mechanism modeling and simulation of basic and acid dyes sorption onto jute fiber carbon: eosin yellow, malachite green and crystal violet single component systems. J. Hazard. Mater. **143**(1), 311–327 (2007)
14. Sivashankar, R.; Sathya, A.B.; Vasantharaj, K.; Sivasubramanian, V.: Magnetic composite an environmental super adsorbent for dye sequestration—a review. ENMM **1**, 36–49 (2014)

15. Luo, X.; Zhang, L.: High effective adsorption of organic dyes on magnetic cellulose beads entrapping activated carbon. J. Hazard. Mater. **171**(1), 340–347 (2009)
16. Shamaila, S.; Sajjad, A.K.L.; Farooqi, S.A.; Jabeen, N.; Majeedand, S.; Farooq, I.: Advancements in nanoparticle fabrication by hazard free eco-friendly green routes. Appl. Mater. Today **5**, 150–199 (2016)
17. Mystrioti, C.; Sparis, D.; Papasiopi, N.; Xenidis, A.; Dermatasand, D.; Chrysochoou, M.: Assessment of polyphenol coated nano zerovalent iron for hexavalent chromium removal from contaminated waters. Bull. Environ. Contam. Toxicol. **94**, 302–307 (2015)
18. Lingamdinne, L.P.; Chang, Y.Y.; Yang, J.K.; Singh, J.; Choi, E.H.; Shiratani, M.; Attri, P.: Biogenic reductive preparation of magnetic inverse spinel iron oxide nanoparticles for the adsorption removal of heavy metals. Chem. Eng. J. **307**, 74–84 (2017)
19. Mart'ınez, C.M.; L'opez, G.M.; Barriada, J.L.; Herrero, R.; Vicente, M.E.S.: Green synthesis of iron oxide nanoparticles. Development of magnetic hybrid materials for efficient As(V) removal. Chem. Eng. J. **301**, 83–91 (2016)
20. Venkateswarlu, S.; Lee, D.; Yoon, M.: Core–shell ferromagnetic nanorod based on amine polymer composite (Fe_3O_4@ DAPF) for fast removal of Pb(II) from aqueous solutions. ACS Appl. Mater. Interfaces **7**(45), 25362–25372 (2015a)
21. Venkateswarlu, S.; Kumar, B.N.; Prathima, B.; SubbaRao, Y.; Jyothi, N.V.V.: A novel green synthesis of Fe_3O_4 magnetic nanorods using Punica Granatum rind extract and its application for removal of Pb(II) from aqueous environment. Arab. J. Chem. (2014). https://doi.org/10.1016/j.arabjc.2014.09.006
22. Venkateswarlu, S.; Kumar, B.N.; Jyothi, N.V.V.: Rapid removal of Ni(II) from aqueous solution using 3-Mercaptopropionic acid functionalized bio magnetite nanoparticles. Water Resour. Ind. **12**, 1–7 (2015b)
23. Venkateswarlu, S.; Lee, D.; Yoon, M.: Bioinspired 2D-carbon flakes and Fe_3O_4 nanoparticles composite for arsenite removal. ACS Appl. Mater. Interfaces **8**(36), 23876–23885 (2016)
24. Venkateswarlu, S.; Minyoung, Y.: Surfactant-free green synthesis of Fe_3O_4 nanoparticles capped with 3, 4-dihydroxyphenethylcarbamodithioate: stable recyclable magnetic nanoparticles for the rapid and efficient removal of Hg(II) ions from water. Dalton Trans. **44**(42), 18427–18437 (2015c)
25. Fazlzadeh, M.; Rahmani, K.; Zarei, A.; Abdoallahzadeh, H.; Nasiri, F.; Khosravi, R.: A novel green synthesis of zero valent iron nanoparticles (NZVI) using three plant extracts and their efficient application for removal of Cr(VI) from aqueous solutions. Adv. Powder Technol. **28**(1), 122–130 (2017)
26. Gupta, V.K.; Nayak, A.: Cadmium removal and recovery from aqueous solutions by novel adsorbents prepared from orange peel and Fe_2O_3 nanoparticles. Chem. Eng. J. **180**, 81–90 (2012)
27. Prasad, K.S.; Gandhi, P.; Selvaraj, K.: Synthesis of green nano iron particles (GnIP) and their application in adsorptive removal of As(III) and As(V) from aqueous solution. Appl. Surf. Sci. **317**, 1052–1059 (2014)
28. Buazar, F.; Baghlani, N.M.H.; Badri, M.; Kashisaz, M.; Khalediand, N.A.; Kroushawi, F.: Facile one-pot phytosynthesis of magnetic nanoparticles using potato extract and their catalytic activity. Starch/Staerke **68**(7–8), 796–804 (2016)
29. Prasad, C.; Yuvaraja, G.; Venkateswarlu, P.: Biogenic synthesis of Fe_3O_4 magnetic nanoparticles using *Pisumsativum* peels extract and its effect on magnetic and Methyl orange dye degradation studies. J. Magn. Magn. Mater. **424**, 376–381 (2017)
30. Shahwan, T.; Sirriah, S.A.; Nairat, M.; Boyacı, E.; Eroğlu, A.E.; Scott, T.B.; Hallam, K.R.: Green synthesis of iron nanoparticles and their application as a Fenton-like catalyst for the degradation of aqueous cationic and anionic dyes. Chem. Eng. J. **172**(1), 258–266 (2011)
31. Ali, I.; Peng, C.; Ye, T.; Naz, I.: Sorption of cationic malachite green dye on phytogenic magnetic nanoparticles functionalized by 3-marcaptopropanic acid. RSC Adv. **8**, 8878–8897 (2018b)
32. Burks, T.; Avila, M.; Akhtar, F.; Göthelid, M.; Lansåker, P.C.; Toprak, M.S.; Muhammed, M.; Uheida, A.: Studies on the adsorption of chromium(VI) onto 3-mercaptopropionic acid coated superparamagnetic iron oxide nanoparticles. J. Colloid Interface Sci. **425**, 36–43 (2014)
33. Nasrazadani, S.; Namduri, H.: Study of phase transformation in iron oxides using laser induced breakdown spectroscopy. Spectrochim. Acta B Mol. Biomol. Spectrosc. **61**(5), 565–571 (2006)
34. Wei, Y.; Fang, Z.; Zheng, L.; Tsang, E.P.: Biosynthesized iron nanoparticles in aqueous extracts of *Eichhornia crassipes* and its mechanism in the hexavalent chromium removal. Appl. Surf. Sci. **399**, 322–329 (2017)
35. Morillo, D.; Uheida, A.; Pérez, G.; Muhammed, M.; Valiente, M.: Arsenate removal with 3-mercaptopropanoic acid-coated superparamagnetic iron oxide nanoparticles. J. Colloid Interface Sci. **438**, 227–234 (2015)
36. Jiang, W.; Wang, W.; Pan, B.; Zhang, Q.; Zhang, W.; Lv, L.: Facile fabrication of magnetic chitosan beads of fast kinetics and high capacity for copper removal. ACS Appl. Mater. Interfaces **6**(5), 3421–3426 (2014)
37. Guan, X.; Chang, J.; Chen, Y.; Fan, H.: A magnetically-separable Fe_3O_4 nanoparticle surface grafted with polyacrylic acid for chromium(III) removal from tannery effluents. RSC Adv. **5**(62), 50126–50136 (2015)
38. Shan, C.; Ma, Z.; Tong, M.; Ni, J.: Removal of Hg(II) by poly (1-vinylimidazole)-grafted Fe_3O_4@ SiO_2 magnetic nanoparticles. Water. Res. **69**, 252–260 (2015)
39. Wang, J.; Zheng, S.; Shao, Y.; Liu, J.; Xu, Z.; Zhu, D.: Amino-functionalized Fe_3O_4@ SiO_2 core–shell magnetic nanomaterial as a novel adsorbent for aqueous heavy metals removal. J. Colloid Interface Sci. **349**(1), 293–299 (2010)
40. Huang, L.; Weng, X.; Chen, Z.; Megharaj, M.; Naidu, R.: Synthesis of iron-based nanoparticles using oolong tea extract for the degradation of malachite green. Spectrochim. Acta A Mol. Biomol. Spectrosc. **117**, 801–804 (2014a)
41. Huang, L.; Weng, X.; Chen, Z.; Megharaj, M.; Naidu, R.: Green synthesis of iron nanoparticles by various tea extracts: comparative study of the reactivity. Spectrochim. Acta A Mol. Biomol. Spectrosc. **130**, 295–301 (2014b)
42. Asad, S.; Amoozegar, M.A.; Pourbabaee, A.; Sarbolouki, M.N.; Dastgheib, S.M.M.: Decolorization of textile azo dyes by newly isolated halophilic and halotolerant bacteria. Bioresour. Technol. **98**(11), 2082–2088 (2007)
43. Ayed, L.; Chaieb, K.; Cheref, A.; Bakhrouf, A.: Biodegradation of triphenylmethane dye Malachite Green by *Sphingomonas paucimobilis*. World J. Microbiol. Biotechnol. **25**(4), 705 (2009)
44. Nidheesh, P.V.; Gandhimathi, R.; Ramesh, S.T.; Singh, T.S.A.: Kinetic analysis of crystal violet adsorption on to bottom ash. Turk. J. Eng. Environ. Sci. **36**(3), 249–262 (2012)
45. Gandhimathi, R.; Ramesh, S.T.; Sindhu, V.; Nidheesh, P.V.: Single and tertiary system dye removal from aqueous solution using bottom ash: kinetic and isotherm studies. Iran. J. Energy Environ. **3**(1), 52–62 (2012)
46. Annadurai, G.; Juang, R.S.; Lee, D.J.: Use of cellulose-based wastes for adsorption of dyes from aqueous solutions. J. Hazard. Mater. **92**(3), 263–274 (2002)
47. Porkodi, K.; Kumar, K.V.: Equilibrium, kinetics and mechanism modeling and simulation of basic and acid dyes sorption onto jute fiber carbon: eosin yellow, malachite green and crystal violet single component systems. J. Hazard. Mater. **143**(1), 311–327 (2007)
48. Ahmad, R.: Studies on adsorption of crystal violet dye from aqueous solution onto coniferous pinus bark powder (CPBP). J. Hazard. Mater. **171**(1), 767–773 (2009)

49. Prasad, A.L.; Santhi, T.: Adsorption of hazardous cationic dyes from aqueous solution onto *Acacia nilotica* leaves as an eco friendly adsorbent. Sustain. Environ. Res. **22**(2), 113–22 (2012)
50. Saha, P.D.; Chakraborty, S.; Chowdhury, S.: Batch and continuous (fixed-bed column) biosorption of crystal violet by *Artocarpus heterophyllus* (jackfruit) leaf powder. Colloids Surf. B Biointerfaces **92**, 262–270 (2012)
51. Chakraborty, S.; Chowdhury, S.; Saha, P.D.: Adsorption of crystal violet from aqueous solution onto NaOH-modified rice husk. Carbohydr. Polym. **86**(4), 1533–1541 (2011)
52. Liang, Z.; Zhao, Z.; Sun, T.; Shi, W.; Cui, F.: Enhanced adsorption of the cationic dyes in the spherical CuO/meso-silica nano composite and impact of solution chemistry. J. Colloid Interface Sci. **485**, 192–200 (2017)
53. Silveira, M.B.; Pavan, F.A.; Gelos, N.F.; Lima, E.C.; Dias, S.L.: *Punicagranatum* shell preparation, characterization, and use for crystal violet removal from aqueous solution. Clean Soil Air Water **42**(7), 939–946 (2014)
54. Önal, Y.: Kinetics of adsorption of dyes from aqueous solution using activated carbon prepared from waste apricot. J. Hazard. Mater. **137**(3), 1719–1728 (2006)
55. Asfaram, A.; Ghaedi, M.; Ghezelbash, G.R.; Pepe, F.: Application of experimental design and derivative spectrophotometry methods in optimization and analysis of biosorption of binary mixtures of basic dyes from aqueous solutions. Ecotoxicol. Environ. Saf. **139**, 219–227 (2017)
56. Mohanty, K.; Naidu, J.T.; Meikap, B.C.; Biswas, M.N.: Removal of crystal violet from wastewater by activated carbons prepared from rice husk. Ind. Eng. Chem. Res. **45**(14), 5165–5171 (2006)
57. Kumar, R.; Ahmad, R.: Biosorption of hazardous crystal violet dye from aqueous solution onto treated ginger waste (TGW). Desalination **265**(1), 112–118 (2011)
58. Zhang, J.X.; Ou, L.L.: Kinetic, isotherm and thermodynamic studies of the adsorption of crystal violet by activated carbon from peanut shells. Water Sci. Technol. **67**(4), 737–744 (2013)
59. El-Sayed, G.O.: Removal of methylene blue and crystal violet from aqueous solutions by palm kernel fiber. Desalination **272**(1), 225–232 (2011)
60. AbdEl-Salam, A.H.; Ewais, H.A.; Basaleh, A.S.: Silver nanoparticles immobilised on the activated carbon as efficient adsorbent for removal of crystal violet dye from aqueous solutions. A kinetic study. J. Mol. Liq. **248**, 833–841 (2017)
61. Ma, W.; Song, X.; Pan, Y.; Cheng, Z.; Xin, G.; Wang, B.; Wang, X.: Adsorption behavior of crystal violet onto opal and reuse feasibility of opal-dye sludge for binding heavy metals from aqueous solutions. Chem. Eng. J. **193**, 381–390 (2012)
62. Smuleac, V.; Varma, R.; Sikdar, S.; Bhattacharyya, D.: Green synthesis of Fe and Fe/Pd bimetallic nanoparticles in membranes for reductive degradation of chlorinated organics. J. Membr. Sci. **379**(1), 131–137 (2011)
63. Haddad, M.E.; Slimani, R.; Mamouni, R.; ElAntri, S.; Lazar, S.: Removal of two textile dyes from aqueous solutions onto calcined bones. J. Assoc. Arab Univ. Basic Appl. Sci. **14**(1), 51–59 (2013)